Return to HTML Version

14

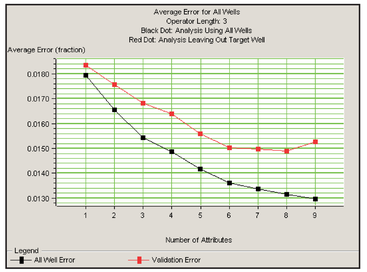

Figure 14: Graph showing the prediction error and validation error for the multiattribute analysis. While the validation error decreases slightly for predictions using 7 and 8 attributes, 6 is determined to be the optimal number in order to avoid overtraining the data.

The attributes used in the porosity prediction were:
RMS amplitude
Perigram
Reflection Strength
Derivative of Instantaneous Amplitude
Integrated Trace
Cosine of Instantaneous Phase

16

a)

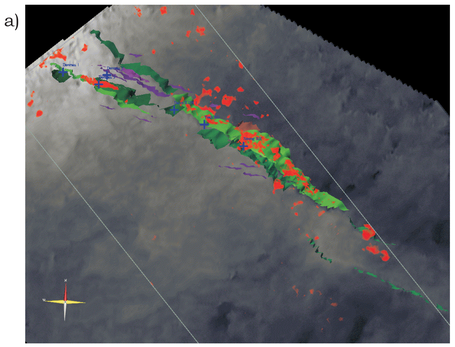

b)

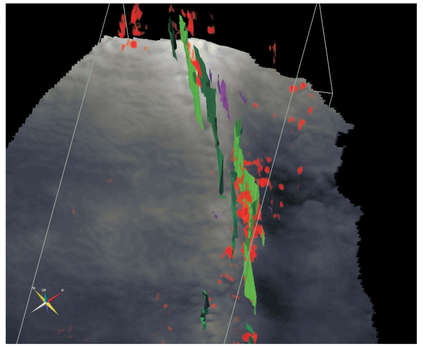

c)

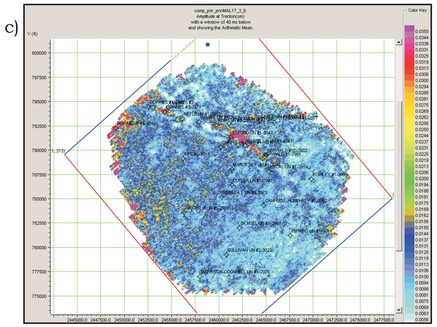

Figure 16:a,b) By exporting the created porosity volume into a program that allowed the faults and seismic to be viewed together in 3-D, it was possible to better visualize the relationship between the faults and the predicted porosity. Values below about 5% porosity were made transparent so that the high porosity (producing) areas could be highlighted. While some noise was predicted by the analysis, c) especially on the edges of the survey, in general the porosity was closely associated with the mapped fault network. The highest porosity values were also concentrated in the areas of intense faulting, especially where the flower structures were located. It was also apparent that although the main fault trend continued at about 122°-302°, the porosity development did not continue with the trend. Instead the porosity was better developed along the NW left lateral step-over fault (Figure 7) that trended at 105°-285°, where there was also a small flower structure

CONCLUSIONS

The Saybrook fault system is consistent with a left lateral strike-slip model, with the main fault movement accommodated by synthetic Riedel shears. Fluid migration may have been aided by the development of antithetic Riedel shears that formed between the overlapping synthetic Riedel shears (flower structures). This hypothesis is supported by the porosity prediction using seismic attributes that illustrated a clear relationship between high porosity values and areas where there were flower structures in the fault zone.

Through the combined use of seismic attributes and fault mapping in 3-D, it is apparent that faulting is one of the key controls on dolomitization, and hence porosity development at the Saybrook Field. For plays similar to Saybrook in which the reservoir development is related to a strike-slip fault environment, detailed fault mapping should help to illuminate the impact these structures had on reservoir development.

REFERENCES

Ahlgren, S.G., 2001. The nucleation and evolution of Riedel shear zones as deformation bands in porous sandstone. Journal of Structural Geology, v. 23, p. 1203-1214.

Ettensohn, F.R., Hohman, J.C., Kulp, M.A., Rast, N., 2002. Evidence and implications of possible far-field responses to Taconian Orogeny: Middle-Late Ordovician Lexington Platform and Sebree Trough, east-central United States. Southeastern Geology, v. 41, p. 1-36.

Hampson, D., Schuelke, J., and Quirein, 2001. Use of multi- attribute transforms to predict log properties from seismic data. Geophysics, v. 66, p. 220-236.

Larsen, G.E., 2000 (Hull, D.N., 1990, chief compiler). Generalized Column of Bedrock Units in Ohio: http://www.ohiodnr.com/geosurvey/pdf/stratcol.pdf.

Mandl, G., 1988. Mechanics of Tectonic Faulting: Models and Basic Concepts. Elsevier: Amsterdam, Netherlands, 407p.

Middleton, K., Coniglio, M., Sherlock, R., Frape, S., 1993. Dolomitization of Middle Ordovician carbonate reservoirs, southwestern Ontario. Bulletin of Canadian Petroleum Geology, v. 41, p. 150-163.

Pearson, R.A., and Hart, B.S., 2004. 3-D seismic attributes help define controls on reservoir development: Case study from the Red River Formation, Williston Basin. In: Seismic Imaging of Carbonate Reservoirs and Systems. G.P. Eberli, J.L. Masaferro, and J.F. Sarg (eds.). American Association of Petroleum Geologists Memoir.

ACKNOWLEDGMENTS

We thank Pete MacKenzie, formerly with CGAS Inc. for supplying the data used in this project. Funding was provided by an NSERC Discovery Grant to Hart. Software was furnished by Landmark Graphics Corp. and Hampson-Russell Software Services.

15

a)

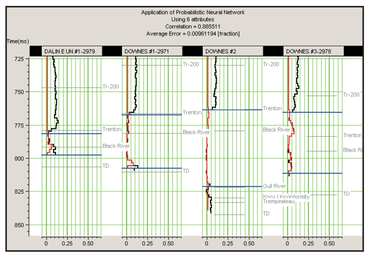

b)

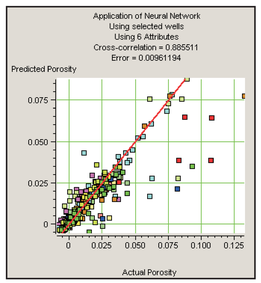

Figure 15: a) The application of the neural network to the training data, the average error was 0.96% and the correlation was 89%. The prediction closely matches the target log (PHIA), except at the bottom of some of the wells where it under-predicted the values. b) Crossplot of the predicted versus the actual values of porosity. The high number of data points is indicative of a volume-based approach, which gives more statistically significant results (Hampson et al., 2001).

17

a)

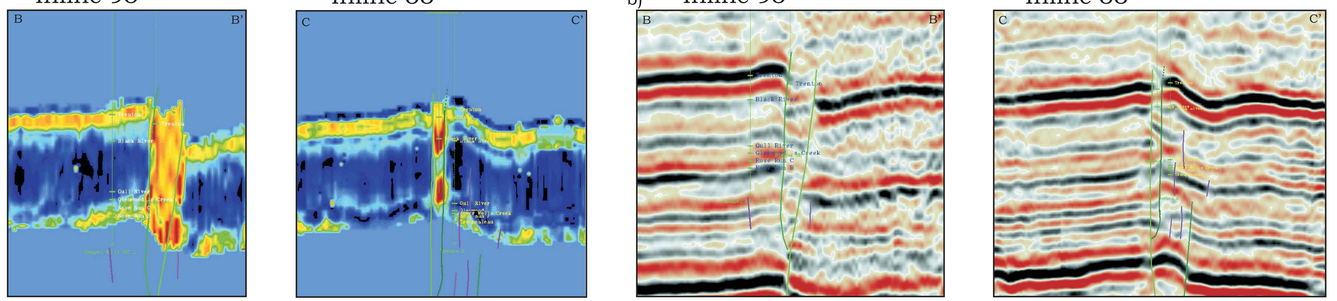

b)

Figure 17: a) Transects through the porosity volume, high porosity is shown in dark reds, while low porosity is in dark blue and black. The volume was only generated for the interval from the top of the Trenton to the Trempealeau horizon. Inline 93 through the porosity volume with Strong UN #1 shown and Inline 33 with the productive Downes #3 on the left and the non-productive Downes #2 on the right. The porosity development is greatest in the areas between the limbs of the flower structures. b) For comparison, the same inlines are shown in the reflection seismic volume.